ChemPubSoc Europe

DOI: 10.1002/ejoc.201700904

EurJOC European Journal of Organic Chemistry

Full Paper

Multi-Step Flow Chemistry

SPECIAL ISSUE

Flow-Assisted Synthesis: A Key Fragment of SR 142948A

Matthew O. Kitching,[a] Olivia E. Dixon,[a] Marcus Baumann,[a] and Ian R. Baxendale*[a]

Abstract: We report a series of multi-step flow operations to deliver an advanced hydrazine intermediate used in the assembly of the neurotensin modulator SR 142948A. Several new reactor configurations have enabled chemical transformations that would be otherwise difficult or dangerous to perform at scale. Overall the flow approach has allowed the preparation of kilogram quantities of the required hydrazine through a short and efficient route.

Introduction

Neurotensin (NT, **1**) is an endogenously expressed tridecapeptide first isolated from bovine hypothalamii in 1973.[1] NT has many roles in regulating numerous biological processes including temperature control,[2] pain sensation,[3] modulation of appetite[4] and pituitary hormone secretion.[5] As a modulator of the body's dopaminergic systems, disruption of NT binding has also been proposed as a possible route to intervention in diseases such as schizophrenia and Parkinson's.[6] Furthermore, upregulation of NT receptor (NTR) expression has been reported to occur in various cancers: lung,[7] breast,[8] pancreas,[9] pituitary[10] and prostate, therefore investigation of its physiological mechanisms is an important area of study.[11] Unfortunately, as a potential therapeutic and investigative tool NT itself has several drawbacks. As a oligopeptide, NT has inherent poor stability in vivo and is degraded by several common endopeptidases and metalloproteases.[12] Its size also prevents easy passage across the blood–brain barrier, which results in poor bioavailability and requires injection of NT directly into the CNS.[13] Finally, NT is only capable of NTR agonism. Consequently synthetically viable, easily modified small molecule probes capable of tailored interaction with the NTR (agonist/antagonist) represent powerful investigatory tools in medicinal chemistry (Figure 1).

As part of our synthetic efforts to prepare a tool box of NT molecular probes, we have already explored the preparation of the NT modulator meclinertant (**2**) by using a flow-chemistry approach.[14] In an extension of this work, we herein disclose efforts towards a synthetically more challenging derivative SR 142948A (**3**).[15] We envisaged a convergent synthesis to allow assembly of this new derivative **3** from three fragments (**4**–**6**, Figure 2), two of which were common to the previous meclinertant synthesis (**4** and **5**) and had already been prepared at scale.[16] The general retrosynthetic disconnection of to the missing fragment **6** is presented in Figure 2, which would ideally be accessed in a multi-step synthesis from the commer-

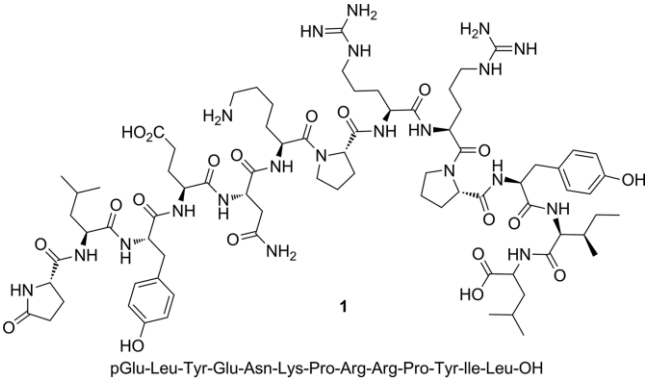

Figure 1. Structures of neurotensin (**1**), meclinertant (**2**), and SR 142948A (**3**).

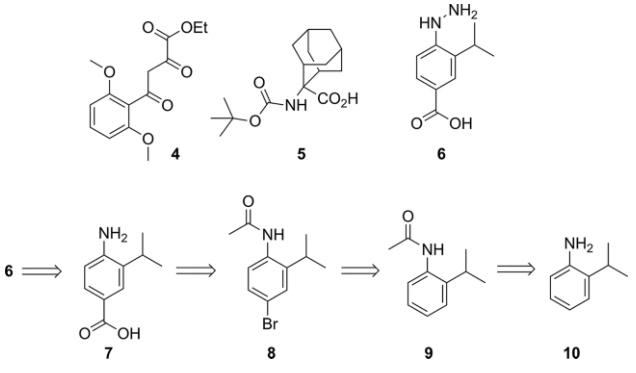

Figure 2. Synthetic fragments of SR 142948A (**3**) and proposed retrosynthesis of hydrazine **6**.

[a] *Department of Chemistry, University of Durham, South Road, Durham, DH1 3LE, UK*
E-mail: i.r.baxendale@durham.ac.uk
https://community.dur.ac.uk/i.r.baxendale/index.html

Supporting information and ORCID(s) from the author(s) for this article are available on the WWW under https://doi.org/10.1002/ejoc.201700904.

cial and readily available starting material 2-isopropyl aniline (**10**).

Results and Discussion

Our strategic approach was to perform an acylation on commercially available isopropyl aniline (**10**), necessary to regulate the subsequent bromination step and furnish selectively intermediate **8**. This would then enable either a cyanation or carbonylation followed by hydrolysis to access the desired carboxylic acid **7**. Diazotization and direct reduction would then yield the corresponding hydrazine product **6**. Although encompassing conceptionally straightforward chemistry, many of these transformations have intrinsic risks associated, especially when conducted at scale such as exotherms (acylation step), or issues due to hazardous (diazotization) or toxic (carbonylation, cyanation) reagents/intermediates. It was anticipated that through the adoption of flow processing techniques, these risks could be managed, minimized or completely avoided.

The initial acyl protection of aniline (**10** → **9**) was associated with a large exotherm when dichloroethane solutions of acetic anhydride (1.73 M; 3 mL/min; 1.1 equiv.) and aniline **10** (1.57 M; 3 mL/min) were combined (Scheme 1). Indeed, at equivalent concentrations the reaction required active cooling to prevent runaway in batch but instead could be easily performed in a microfludic mixing chip as a flow process, which ensured good thermal transfer to the surrounding environment. In this way, the solution could be continuously processed while maintaining a temperature <55 °C. Beneficially, it was discovered that the following bromination step (**9** → **8**) required heating to achieve complete conversion. By creating a sandwich assembly from two additional mixing chips (inputs for the *N*-bromosuccinimide) in direct thermal contact with the first acylation reactor, the excess heat produced in the acylation could be used in a productive fashion to prewarm the reaction media for the second step (Figure 3).[17]

The reaction stream from the first acylation step was therefore split and directly combined with input streams containing NBS in dichloroethane (DCE, 0.94 M; 3 mL/min in two parallel channels; 1.2 equiv.) (Scheme 1). The two flow streams were reunited and then passed through further residence time coils (4 × 52 mL) maintained at 70 °C to ensure complete bromination. The reaction mixture was quenched and an in-line work-up was performed (through two parallel streams) by mixing with a stream of basic sodium sulfite and separated by using a mixer-settler membrane unit. The device was constructed around a Biotage universal separator,[18] which allowed the bifurcation of the organic product containing phase and the aqueous waste (Figure 4).[14a,19] Run as a continuous process, this allowed the isolation of the amide product **8** by direct evaporation of the DCE. In total, over 120 L of organic solution was processed in a continuous operation over the course of 167 h (ca. seven days), thus generating an isolated mass of 11.52 kg of product equating to 96 % yield. Furthermore, we were able to establish a refilling schedule for the input stock solutions (2.5–5 L batches) based upon their consumption flow rates that enabled the efficient recycling of recovered DCE from the final evaporation stage. Consequently the process only required the use of 26.7 L of DCE amounting to a significant reduction in the amount of organic solvent used.

With kilogram quantities of the bromide **8** in hand, further derivatization to the corresponding nitrile **11** was undertaken by employing a palladium-catalyzed approach (Scheme 2).[20] These experiments were evaluated by using an automated microwave setup. Initial investigation of reaction conditions showed the importance of including a reductant in the reaction

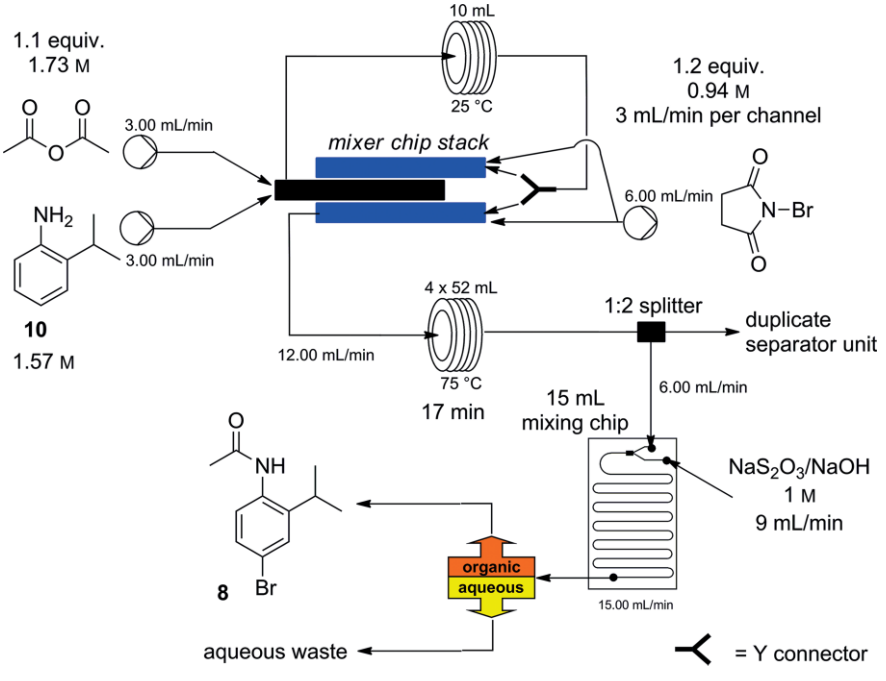

Scheme 1. Flow-reactor schematic for the synthesis of brominated amide **8**.

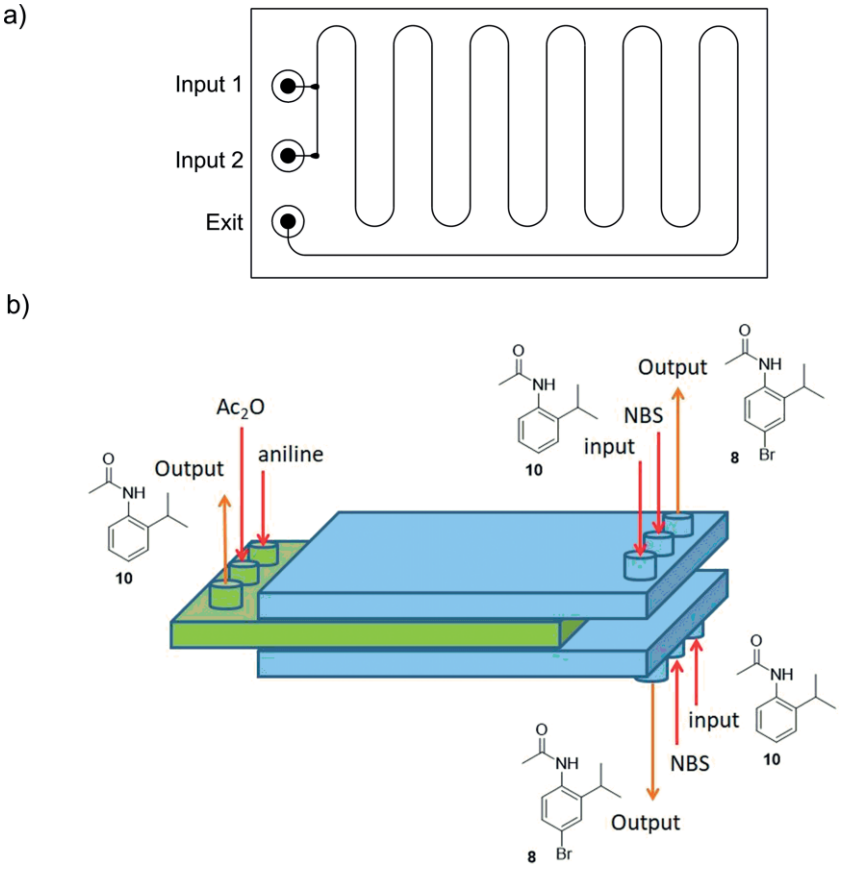

Figure 3. a) Single-layer microfluidic chip. b) Sandwich-chip device for thermal transfer between reaction steps.

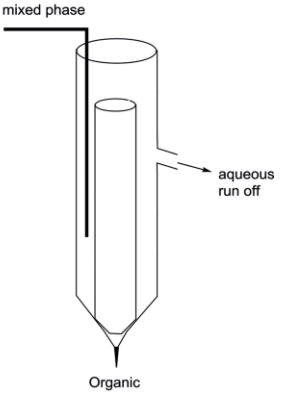

Figure 4. In-line extractor used for organic–aqueous separation.

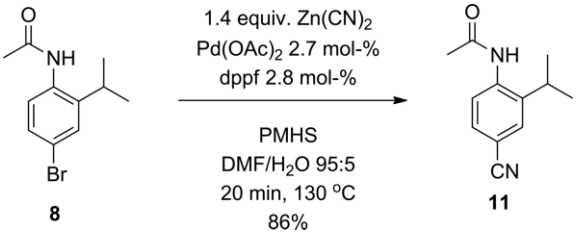

Scheme 2. Optimized batch conditions for synthesis of nitrile compound **11**.

mixture (Table 1: entries 1–4). In the absence of poly(methylhydrosiloxane) (PMHS),[21] no conversion was observed with either supported or solution-phase catalysts. Screens of common supported forms of palladium (Table 1; entries 5, 6, 8, and 9) showed lower conversion and extended reaction times compared to the use of solution phase palladium(II) acetate. A solvent screen determined that a mixture of DMF/H_2O (95:5) gave optimal results.

To process material on a semi-preparative scale, the automated microwave reactor was utilized as a sequential batch process reacting 39 mmol of substrate and allowing 6.8 g of nitrile **11** to be isolated in 86 % yield. Although this approach was convenient for small laboratory-scale preparation to generate sufficient material for further scoping studies, the observed low solubility of the reagents (only becoming soluble as the reaction progressed) led us to conclude that this would be a difficult reaction to translate to continuous flow and therefore alternative approaches were sought.

The possibility of performing a carbonylation reaction continuously was next investigated. Again, the initial investigation and optimization work was conducted using an automated microwave setup. The use of microwave vials allowed easy introduction of CO gas and pressurization of the reaction mixture up to 5 bar. Both ethanol and methanol could be successfully

Table 1. Optimization of microwave cyanation conditions..

Entry	Catalyst[a]	Temp [°C]	Additive	Solvent[c]	Time [h]	^{1}H NMR conversion [%]
1	$Pd(OAc)_2$	80	dppf/PMHS	DMF/H_2O	3	66
2	$Pd(OAc)_2$	80	dppf	DMF/H_2O	3	0
3	$Pd(OAc)_2$ EnCat[b]	80	dppf/PMHS	DMF/H_2O	3	74
4	$Pd(OAc)_2$ EnCat[b]	80	dppf	DMF/H_2O	3	0
5	$Pd(OAc)_2$/dppf EnCat[b]	80	PMHS	DMF/H_2O	3	6
6	Pd-NP EnCat	80	dppf/PMHS	DMF/H_2O	3	77
7	$Pd(dba)_2$	80	dppf/PMHS	DMF/H_2O	3	78
8	$Pd(OAc)_2$ Chemdose	80	dppf/PMHS	DMF/H_2O	3	5
9	$Pd(OAc)_2$ EnCat	80	dppf/PMHS	DMF/H_2O	3	57
10	$Pd(OAc)_2$	120	dppf/PMHS	DMF/H_2O	1	> 98
11	$Pd(OAc)_2$	120	dppf/PMHS	*i*PrOH/H_2O	2	73
12	$Pd(OAc)_2$	120	dppf/PMHS	MeCN/H_2O	2	63
13	$Pd(OAc)_2$	120	dppf/PMHS	1,4-dioxane/H_2O	2	75
14	$Pd(OAc)_2$	120	dppf/PMHS	H_2O	1	69
15	$Pd(OAc)_2$	120	dppf/PMHS	DMF	1	87
16	$Pd(OAc)_2$	120	dppf/PMHS	*i*PrOH	2	78
17	$Pd(OAc)_2$	120	dppf/PMHS	1,4-dioxane	2	75
18	$Pd(OAc)_2$	120	Xantphos/PMHS	DMF/H_2O	1	> 98

[a] Standard loading 2.2 mol-%. [b] Loading 4.4 mol-% based upon Pd loading. [c] Solvent ratio 95:5.

used in the transformation; however, ethanol showed the highest conversion while minimizing the amount of protodehalogenation (as determined by ^{1}H NMR analysis of the crude reactions).

By using the microwave automation a sequential run of ten reactions allowed the processing of the bromide **8** on a 59 mmol scale to generate 12 g of material in 81 % isolated yield (Scheme 3). Additionally, it was observed that the yield for each run was consistent (indicating catalyst/substrate stability over time), and the reaction mixtures remained essentially homogeneous throughout the processing (some indication of Pd black formation was noted). This immediately allowed us to consider translation of the conditions to a flow based system.

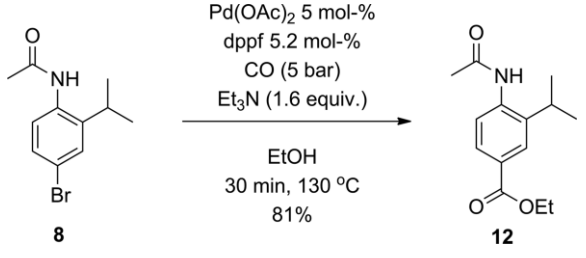

Scheme 3. Optimized batch conditions for synthesis of ester **12**.

The direct introduction of CO gas at high pressure to perform carbonylation chemistry has been widely demonstrated by using several designs including simple tube-in-tube systems.[22] However, although the handling and introduction of high-pressure gases to flow systems is achievable, safety restrictions may prevent the use of high-pressure CO – as was the case for ourselves. As such, the final design of our flow system was restricted to a low-pressure CO-injection system and shows certain engineering features that are worth highlighting as they can be easily adopted to solve related issues commonly encountered in other fields, for example the introduction of semi-volatile amines.

The configuration of the flow reactor used is depicted in Scheme 4. The system consisted of a mixing chip fed by an ethanolic solution of the substrate, catalyst and base to be blended with a low-pressure input (3 bar, 2.5 mL/min) of CO-regulated through a flow meter.[23] A plug flow regime was generated and used directly as the feed for a HPLC pump.[24] The pump was used to upregulate the pressure to 10 bar, which makes the reaction mixture homogeneous and delivers sufficient CO for efficient carbonylation in the subsequent coil-reactor stage (Polar Bear Plus[25] ca. 37 min; 120 °C). It was noted that during the reaction, colloidal palladium particles formed in the coil reactor (additives like tetraalkyl ammonium salts, DMF and alternative metal chelating ligands were investigated but failed to have any effect on the process). This gave no issues with reactor blocking through aggregation with the particulates being efficiently progressed through the reactor even over prolonged reaction periods. However, clogging of the in-line back-pressure regulator (BPR), required to maintain the system pressure, rapidly occurred. In addition, significant and uncontrolled degassing was also an issue at the exit of the reactor; this was made more problematic due to the particulates in the system, which were explosively jettisoned from the flow stream leading to etching of the collecting vessel and creating containment problems.

To overcome both of these issues, we constructed a simple membrane partitioned sedimentation tank, which also acted as a controlled gas exhaust. The unit was constructed from a stainless-steel pressure chamber with an embedded thermocouple and pressure dial. An adjustable pressure release valve was fitted into the cap to enable controlled discharge of the CO gas.[26] In our first assembly, the input feed delivered the solution and particulates from the reactor into the sedimentation chamber and the exit line was fitted with a polytetrafluoroethene (PTFE) solvent filter (see the Supporting Information).[27] This output line was connected as a feed to an HPLC pump, which progressed the filtered product solution through the scavenging column. Although this approach worked well over

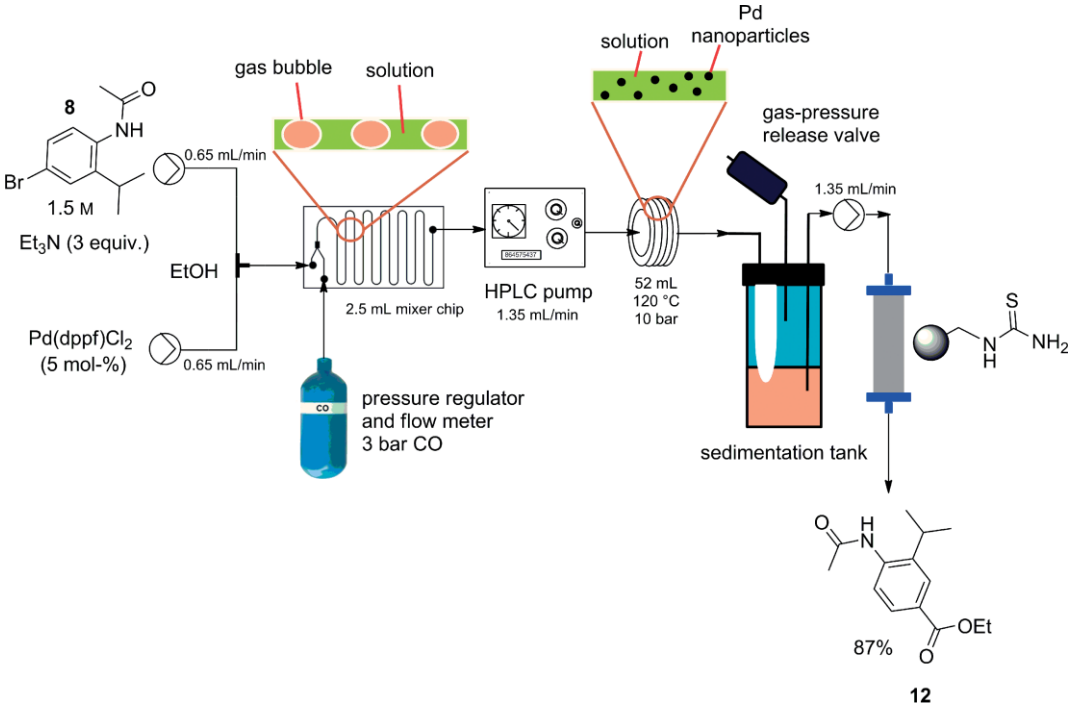

Scheme 4. Flow-reactor design for carbonylation leading to ester **12**.

short processing times, we noticed that build-up of the particulate material around the in-line PTFE solvent filter started to impair the pumping efficiency of the exit HPLC pump by restricting its input flow. This was easily observed by noting the decline in the flow rate of the exit solution, indeed, HPLC systems are well known for having very little tolerance on the pressure drop of the input line. We found that by alternatively using a extraction thimble filter[28] fitted at the inlet of the sedimentation chamber and utilizing the pressure drop from the reactor more effective, filtration of the particulate matter could be achieved. In this way, the pressure feed of the solvent for the exiting HPLC remained constant. The reactor could be run for up to 8 h before particulate build-up required a scheduled shutdown and exchange or cleaning of the thimble filter. Finally, the solution pumped from the sedimentation tank was directed through a column of QP-TU (a thiourea functionalized resin) to remove residual metal contaminants before batch collection and solvent evaporation. The crude product was directly triturated with a mixture of water/ethanol (20:1) and filtered. The tan-coloured solid was air-dried to yield the desired ester product in excellent purity as assessed by ^{1}H NMR and LC-MS. During a typical 8 h run, 120 g of starting material could be processed in 87 % isolated yield equating to a productivity of 12.7 g/h (58.5 mmol/h).

Although delivering high-quality material, this approach did not fulfil our target throughput requirements for a continuous process and was uneconomic due to the high loading and associated cost of the palladium and dppf ligand. We therefore sought other approaches; a strategy which offered simplicity and directness seemed to be a Sonogashira coupling followed by an oxidative cleavage of the acetylene to furnish a carboxylic acid moiety (Scheme 5).

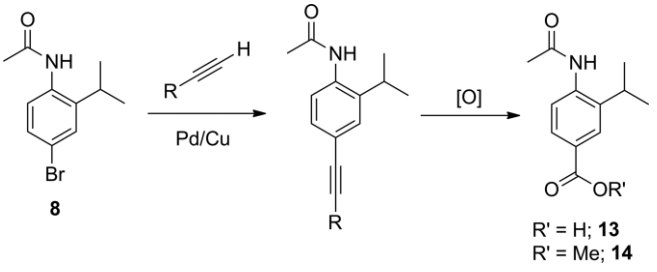

Scheme 5. New strategic approach to the target structures **13** and **14**.

We initially performed a scope evaluation on the Sonogashira reaction by using a series of automated microwave reactions systematically assessing catalysts (palladium and copper sources), bases, solvents, concentration/stoichiometry, temperature and reaction times. All reactions were rapidly assessed as % conversion by using calibrated LC-MS analysis (a summary of the findings appear in the Supporting Information). From this study, a set of optimum conditions (90 % isolated after column chromatography) were defined that seemed to also favour translation of the reaction to a flow processing regime (Scheme 6). We were also able to demonstrate that in the presence of a basic solution of RuO_2 and the co-oxidant $NaIO_4$ (or oxone), oxidative cleavage of the alkyne occurred (3.5 h) to give 94 % isolated yield of the corresponding carboxylic acid product **13**.[29]

Based upon these findings we embarked upon the translation of the Sonogashira step to flow.[30] First however, an additional incubation study (48 h) was performed where the different reaction components were tested for their stability, compatibility and prolonged solubility in different combinations (see

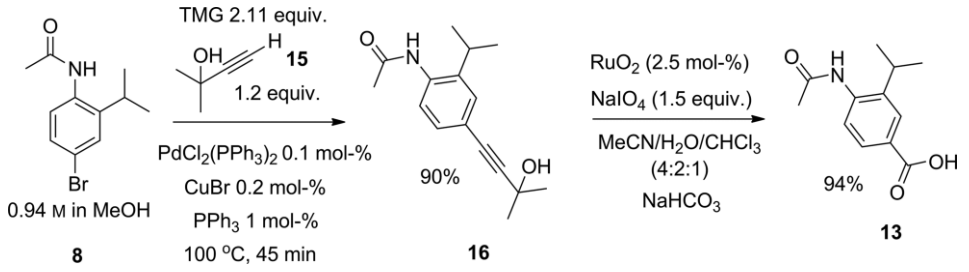

Scheme 6. Optimized conditions for microwave Sonogashira coupling reaction and oxidative cleavage of the alkyne group.

the Supporting Information). This was conducted to ensure that stable stock solutions of the components could be prepared to enable prolonged processing without constant manual intervention. From this investigation, a simple two-channel flow set-up was conceived; channel A, delivered a flow stream comprising of the aryl bromide **8** (2.5 M), the TMG base and the CuBr in MeOH (Scheme 7); channel B, a methanolic solution of the propargylic alcohol (3 M), palladium catalyst and associated PPh_3 ligand. The two streams (1:1 flow rate of 1 mL/min) were united at a simple T-piece mixer before progressing into a heated coil reactor (two conjoined 52 mL Polar Bear plus systems) maintained at 100 °C (microwave optimized temperature) with a 250 psi BPR used to maintain the system pressure. The exiting solution indicated a steady-state conversion of 93 %, which could be driven to complete conversion by simply raising the reactor temperature to 105 °C. This gave a theoretical throughput of 0.15 M/h or 38.9 g/h. The product could be readily isolated by evaporation of the solvent and pouring the resulting crude oil obtained into a stirred solution of 3 M HCl (0 °C). The product precipitated over the course of approximately 1 h and could be filtered and dried at 40 °C under vacuum to give an overall isolated yield of 93 % (5 h run). To demonstrate the robustness of the system, a continuous run over five days was performed to collect the reactor output into individual batches, which equated to daily production, which were then manually worked up. Overall a yield of 90 % with a deviation of +3.7 % was obtained, which equated to a total of 4.2 kg of isolated material.

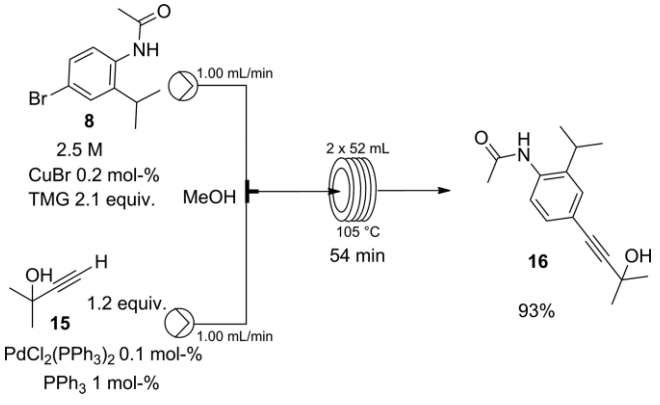

Scheme 7. Flow Sonogashira coupling reactor.

It was our initial intention to attempt direct oxidation of the acetylene product **16** without work-up and isolation. However, we found that attempts to directly use solutions of the reactor output under the previously attempted oxidation conditions (RuO_2/$NaIO_4$) inevitably gave an alternative major dibrominated adduct **17** (Scheme 8). Presumable, this product formed through preferential oxidation of bromide (carried TMG•HBr salt), which generates in situ bromine, which adds to the alkyne leading to **17** through hydrolysis.[31] This was partially confirmed by demonstrating that when basic (K_2CO_3) solutions of acetylene **16** in 1:1 solutions of MeOH/H_2O were treated with bromine the identified product **17** rapidly formed. As all related oxidation processes would potentially generate the same difficulties, we investigated adding an additional purification stage.

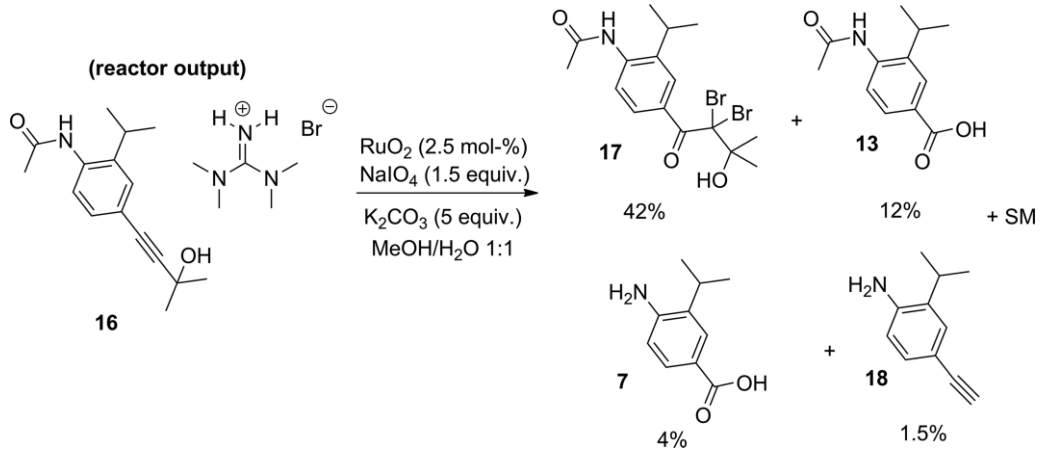

Scheme 8. By-product formation in the oxidation of acetylene **16**.

To achieve the reaction stream clean-up we elected to employ a dual-stage scavenging process (Scheme 9) to first utilize a cartridge of Ambersep 900 OH resin (Columns A–E), to neutralise the TMG•HBr salt, followed by a second cartridge of a sulfonic acid resin (QP-SA, Columns F–J), which sequestered the free TMG base. Although a mixed bed of the two resins was also effective, we found it much more efficient to stage the scavenging sequence as this helped in constructing a simple automated column-exchange process, which enabled interchange of the two types of scavenging columns as they became depleted. Introduction of replacement columns and ensuring the washing/regeneration of depleted units was conducted by a simple multi-port valve system as described previously.[32] For this process we set the unit to trigger based upon a timing event to correspond to the sequestering threshold of the various packed columns as calculated from the flow rate and theoretical concentration of the TMG input. This generated a flow stage as depicted in Scheme 9.

Although this in-line work-up was effective, we were still unable to achieve an efficient oxidative cleavage of the alkyne (< 42 % conversion) without first effecting a solvent swap to the original acetonitrile/water/$CHCl_3$ mixture. As we desired to produce a telescoped sequence by linking the oxidation to the Sonogashira step, we decided to explore more amenable strategies.

There are only limited studies in the literature regarding the ozonolysis of alkynes.[33] In addition, there is no clear view as to which substrates yield anhydride or carboxylic acid products valuable for our study and which substrates result in benzil derivatives, which would be of less use.[34] We however thought it would be of speculative interest to evaluate the transformation with regard to our particular substrate **16**. We aimed to make use of the fact that the ozonolysis reaction could be performed in an alcoholic solvent to, in theory, aid the breakdown of the ozonide intermediates and fragment the intermediate anhydrides if produced. Ultimately, we wished to perform the ozonolysis directly on the methanolic reactor output used in the preparation of **16** (Scheme 7). Several flow reactors have been reported for ozonolysis reactions,[35] however, we elected to use a simple wavy annular flow[36] ozonolysis design,[16b] which we had previously employed successfully at scale (Scheme 10). This used a simple T-assembly to inject a flow of substrate **16** from a capillary input into a fast flowing gas flow of the O_3 reactant.

From the initial ozonolysis runs we were pleased to identify the oxidative fragmentation products **13**, **14**, **7** and **21** and small amounts of 2-hydroxy-2-methylpropanoic acid **19** as well as the corresponding methyl ester adduct **20**. Table 2 summarizes some of the further informative optimization results. As can be seen, temperature controls the distribution of aryl products through direct and secondary hydrolysis, however, it has a nominal influence on conversion. Concentration and residence time were found to be the main parameters determining starting-material consumption. The addition of additives such as acids

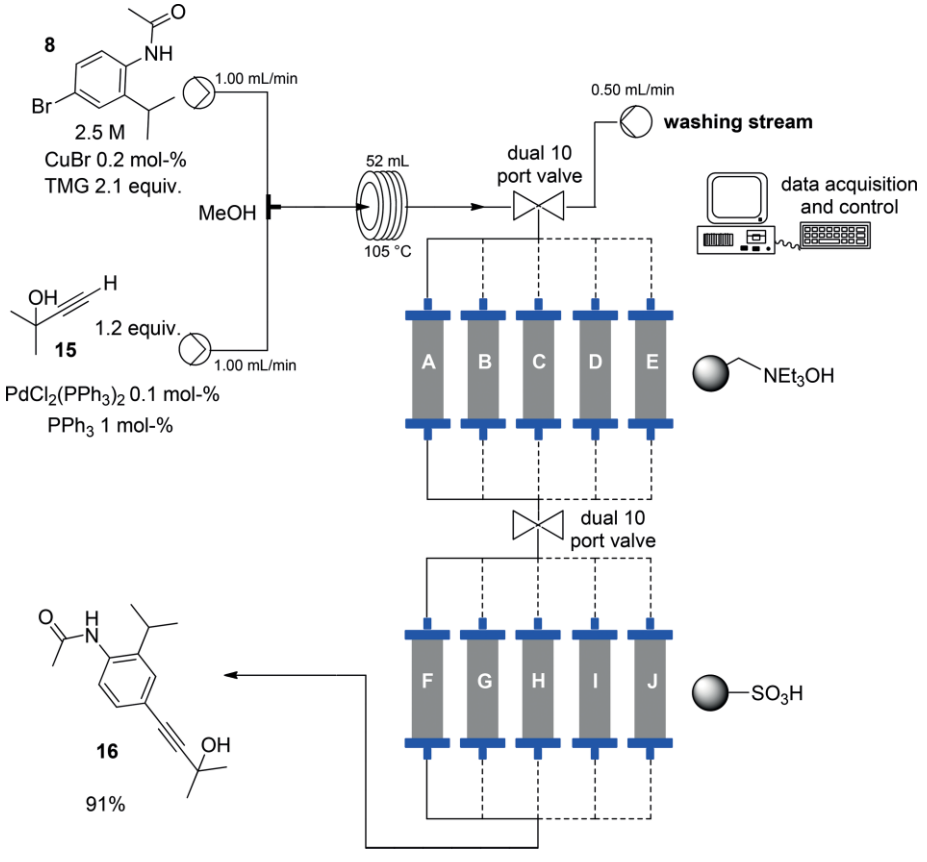

Scheme 9. Flow process for the synthesis of acetylene **16**.

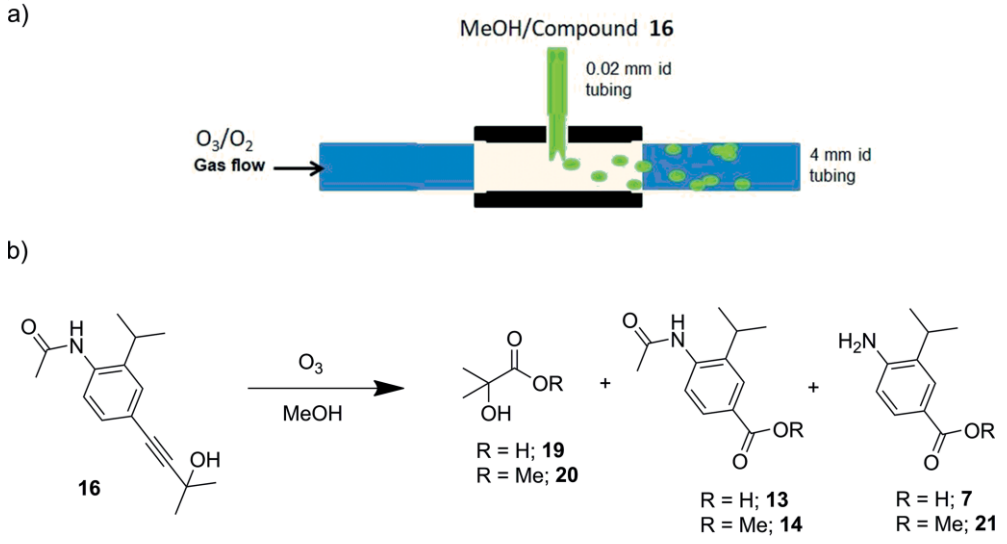

Scheme 10. a) Flow ozonolysis of acetylene **16**. b) Products derived from the flow ozonolysis.

(e.g. HCl, PTSA) or bases (pyridine, DMAP, K_2CO_3) neither enhance conversion nor reaction rates and had only small effects on product proportions.

Table 2. Subset optimization of flow ozonolysis reaction conditions.

Ent.	Oxygen flow rate[a]	Substrate flow rate[b]	Temp °C	Conv. %	Ratio[f] **13:14:7:21**
1	1.0	1.0	0	100	15:79:2:4
2	1.5	1.5	0	90	13:83:2:2
3	2.0	1.5	0	100	11:86:1:2
4	3.0	2.0	0	86	10:88:1:1
5	4.0	2.0	0	74	9:89:1:1
6	2.0	1.5	–78	100	2:98:0:0
7	2.0	1.5	r.t.	100	19:73:3:5
8	2.0	1.5[c]	r.t.	97	18:72:4:6
9	2.0	1.5[d]	r.t.	73	Nd
10	2.0	1.5[e]	r.t.	64	Nd
11	2.0	1.25[e]	r.t.	82	Nd
12	2.0	1.0[e]	r.t.	96	18:74:2:6
13	2.0	0.75[e]	r.t.	100	19:76:3:5
14	2.0	0.85[e]	r.t.	100	18:76:3:3
15	2.0	0.95[e]	r.t.	96	17:76:3:4

[a] O_2 flow rate was controlled by using a Brukhurst flow meter. [b] 0.5 M in MeOH. [c] 0.7 M in MeOH. [d] 0.9 M in MeOH. [e] 1 M in MeOH. [f] As determined by UV-LC rounded to nearest %. Nd = not determined.

For the final flow process we elected to use a concentration of 1 M and flow rates of 2 and 0.85 mL/min for the oxygen and substrate streams, respectively; at ambient temperature this gave quantitative conversion. This additionally produced a good match for the concentration of the exiting stream from the Sonogashira step. Although the oxidation of alkynes to anhydrides avoids the production of classical intermediates such as ozonides and peroxides, upon analysis the processed solution still contained low levels of peroxy species (≈ 10 mg/L).[37] To aid decomposition of these residual peroxy species a short packed column of MnO_2 was added in-line, which reduced the amount of peroxy components below detectable levels. Overall, a processing capacity of 51 mmol/h was achieved which would equate to approximately 12 g/h of product. Figure 5 shows a representative ^{1}H NMR spectrum of the crude reaction mixture directly following evaporation of the output stream. The final

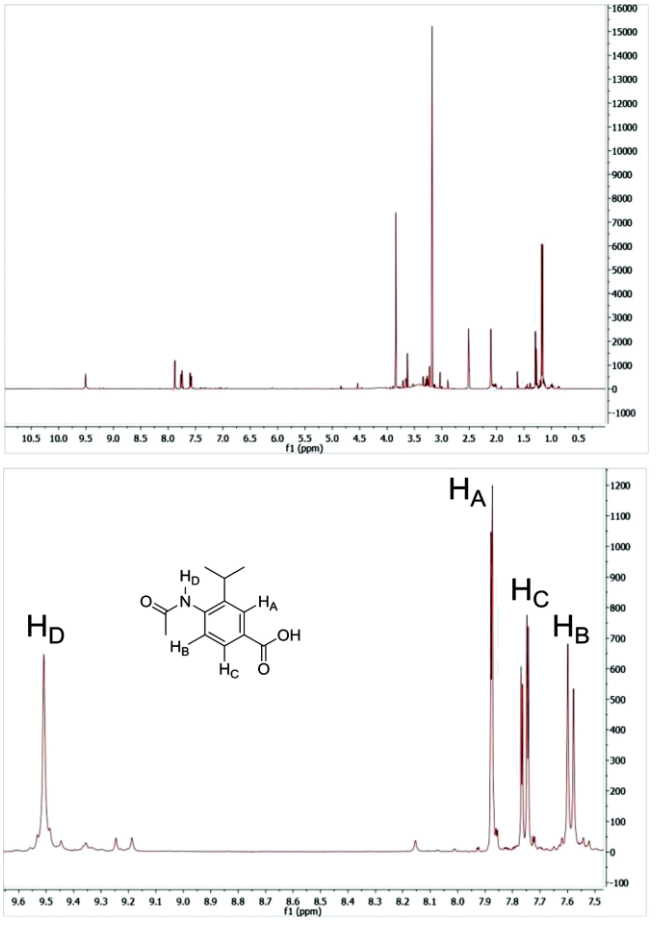

Figure 5. (top) ^{1}H NMR of the crude reaction from ozonolysis – entry 2 Table 1 and (bottom) the expansion of the aromatic region of the same spectra. 400 MHz in [D_6]DMSO.

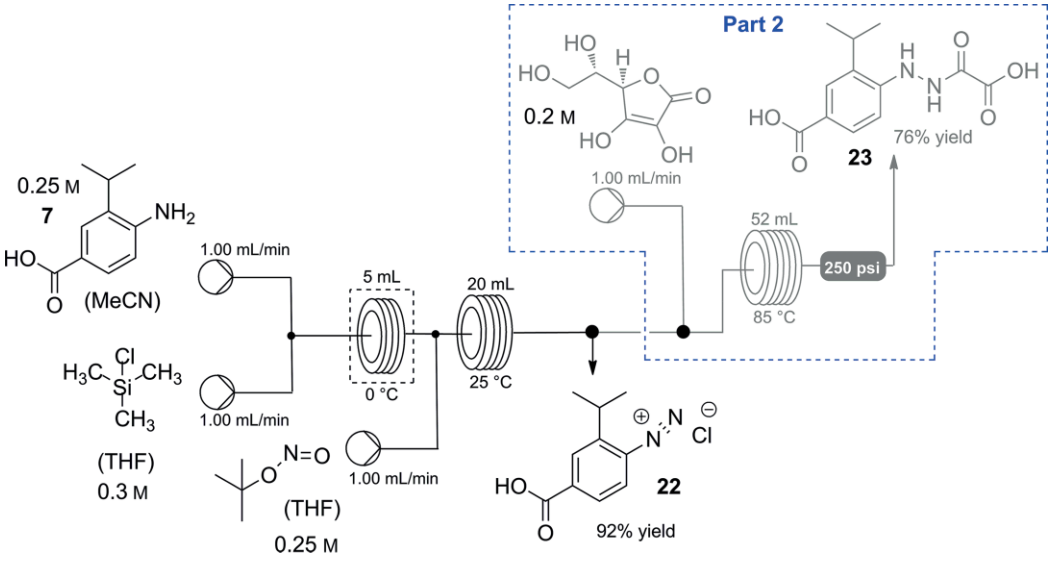

Scheme 11. Flow diazotization of aniline **7** and part 2 ascorbic acid reduction.

product could be isolated by solvent evaporation and allowed the crude product to crystallize upon standing in a 65 % yield after filtration and washing with cold hexane. The corresponding carboxylic acid **7** could be obtained quantitatively by heating the same crude material dissolved in 3 M HCl at 125 °C for 30 min by passage through a tubular flow coil reactor. As these acidic conditions met our need for the subsequent sequence, we anticipated using this solution directly in the next operation.

To access hydrazine **6** would require a further two-step sequence of diazotization and reduction. Here we were able to rely on some previously devised flow chemistry involving reaction of a diazonium salt generated in situ[38] with ascorbic acid to affect the reduction (Scheme 11).[39] As an alternative and backup approach we also evaluated a more classical reduction involving a mixture of $SnCl_2$ and HCl, which was shown to work well in batch.

To evaluate the transformation of aniline **7** to its hydrazine derivative **6**, we initially started with isolated and purified material (Scheme 11 – initially excluding part 2). A bulk solution of 4-amino-3-isopropylbenzoic acid (**7**) was prepared in acetonitrile and pumped at a flow rate of 1.00 mL/min to combine with a second solution of trimethylsilyl chloride in THF also with a flow rate 1.00 mL/min. The combined flow was directed into a short 5 mL FEP (fluorinated ethylene propylene copolymer) reactor coil, which was maintained at 0 °C (2.5 min residence time). The exiting stream was further combined with a THF solution of *tert*-butyl nitrite (flow rate 1.00 mL/min) and reacted in a 20 mL FEP coil at room temperature (6.5 min residence time). A precipitate formed during the reaction, which was collected at the exit of the reactor by filtration to give the diazonium salt **22** in an excellent 92 % isolated yield.

To extend this sequence (Scheme 11 – reactor part 2), we incorporated a further pump to deliver an aqueous stream of the ascorbic acid reductant (flow rate 1.00 mL/min) and passed the flow stream into a coil reactor (52 mL Polar Bear Plus,[28] 85 °C - 13 min residence time). A 250 psi BPR was used to maintain the system pressure. During passage through the heated reactor, the solution became homogeneous and was collect at the reactor exit. A batch work-up was then used to extract the corresponding oxamic acid **23** to evaluate the effectiveness of the sequence.[40] First, the output solution was diluted with ethyl acetate and extracted with 2 M NaOH (pH 10–11). The aqueous extract was separated, reacidified and back-extracted into EtOAc. The solid material obtained from evaporation of the solvent was crystallized from a 7:1 mixture of THF/Et_2O to yield the hydrazine adduct **23** in 76 % yield as a pale yellow solid.

After having set a benchmark with the ascorbic acid approach, we next evaluated the alternative tin-mediated process as shown in Scheme 12. Again, by using a simple three-pump system, this time based upon a peristaltic delivery system (Vapourtec E-Series Flow reactor[41]), a solution of the aniline **7** in a 1:2 mixture of HCl and AcOH (0.2 M) was mixed with a solution of aqueous $NaNO_2$ (1.3 M) at a T-piece (PTFE: polytetrafluoroethylene). The mixture was then directed through a FEP flow-coil reactor maintained at 0 °C (2.8 min residence time). A further flow stream containing the $SnCl_2$ in HCl (0.55 M) was united and the mixture passed into a second heated FEP flow coil (52 mL, 40 °C, Polar Bear Plus[28] – 23 min residence time). A suspension rapidly formed but could be easily propagated through the reactor without causing blockage. The reactor output was dispensed directly onto a sintered filter. After 60 min of operation, the filter cake was washed with water to give 3.48 g, 84 % isolated yield of the hydrazine salt **24** after drying.

The success of the aqueous conditions for the diazotization in this latter transformation and the environmental benefits of the ascorbic acid reduction prompted us to attempt to assimilate the two processes to furnish an improved protocol. We also wished to try and telescope the previous acid-mediated hydrolysis of the protected aniline **14** to its corresponding amino compound **7** into this new assembly. We therefore devised the modified setup as depicted in Scheme 13.

Taking the crude solution of ester **14** (still with **19** and **20** present) as the starting point, we carried out the hydrolysis un-

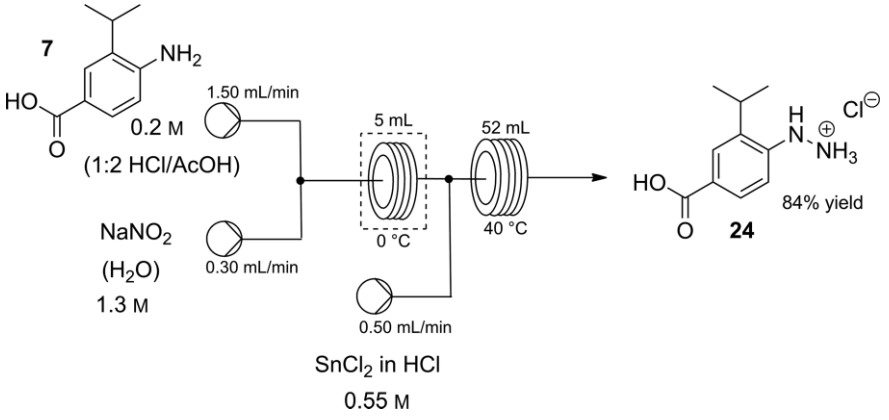

Scheme 12. Flow diazotization and Sn-mediated reduction starting from acid aniline **7**.

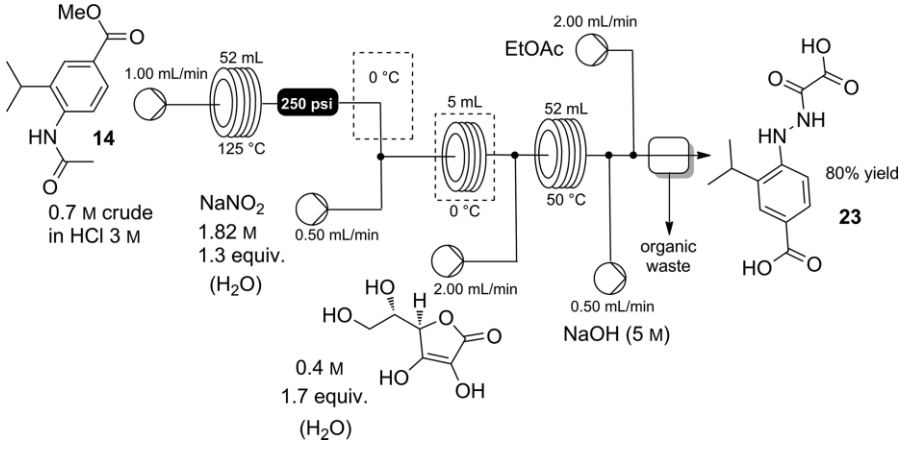

Scheme 13. Telescoped synthesis of hydrazine adduct **23**.

der the previously determined acidic conditions (Scheme 13). The processed flow stream then passed through a cooling zone before next being mixed with an aqueous solution of $NaNO_2$ and entering a short residence-time flow coil (FEP 5 mL) maintained at 0 °C. This flow stream, containing the intermediate diazonium, was immediately combined with the reducing ascorbic acid solution, and the resulting hydrazine ester adduct, which formed in situ was digested as it passed through a heated flow coil furnishing the oxamic acid **23**. To facilitate a partial workup, a quench solution of NaOH was first injected into the flow to generate a basic solution followed by an input of EtOAc to form a biphasic flow. The organic- and product-containing aqueous streams were at this stage phase separated by using the previously described in-line extractor (Figure 4). This resulted in isolation of a basic solution of the oxamic acid product **23** that could be subsequently isolated by careful acidification and extraction (of particular note was that the more aqueous soluble acid **19** was not found as a contaminant in the product[42]).

As a proof of concept, we were also able to demonstrate that this final acidification and extraction could also be achieved as a flow sequence, again by utilizing the in-line separator. However, in practice it was found more efficient to simply batch the product solution and acidify this in bulk prior to extraction.

Pleasingly, we achieved a reliable isolated yield of compound **23** in 80 % both for short reactor runs (1–3 h) and over prolonged usage (full-day runs of 8–10 h). This enabled a reasonable productivity of 34 mmol/h that delivered over 8.9 g/h for the integrated four-step transformation.

Finally, in the context of this project, we exemplified that the target hydrazine adduct **23** could be successfully utilized in the desired reaction with fragment **4** under thermal conditions to synthesize pyrazole **25** (Scheme 14). This was achieved by heating a solution of compounds **4** and **23** in 1,4-dioxane in the presence of 10 mol-% *p*-TSA at 120 °C for 2.5 h. The reaction gave an 86 % isolated yield of **25** after work-up and purification by column chromatography.

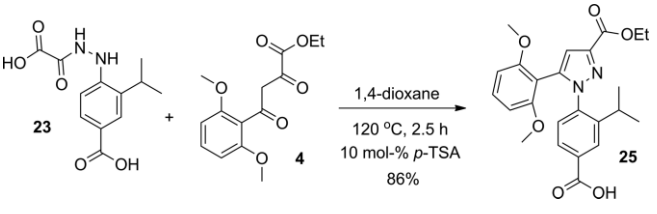

Scheme 14. Preparation of pyrazole **25** by batch microwave synthesis.

Conclusions

In this work we have developed a set of multi-step flow sequences starting from readily available aniline **10** to an advanced hydrazine derivative **23**. The route generated has a number of staging points were natural breaks in the processing allow the batching of intermediates, in each case as bench stable solids (Figure 6). As part of our flow-processing strategy we have made use of some established flow transformations (e.g., diazotization and reduction) as well as developed new chemistries (e.g., selective ozonolysis of an alkyne). This has generated several improvements with regards to solvent usage (synthesis of **8** and telescoping **16** → **14**), energy utilization (synthesis of **8**) and the number of required reaction steps. Ultimately we have been able to create a set of linked flow operations, which deliver high quality material with good productivity (Figure 6). By employing this chemistry, we have successfully generated 4.27 kg of the final hydrazine derivative **23** for use in the synthesis of SR 142948A (**3**) and other important derivatives.

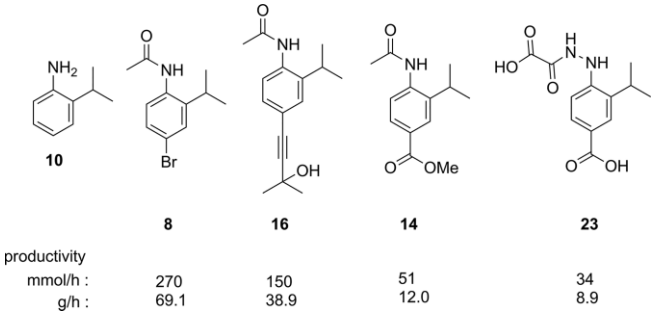

Figure 6. Key intermediates and outputs for the flow synthesis towards compound **23** a synthetic equivalent of target hydrazine **6**.

Experimental Section

For protocols and reactor descriptors see the Supporting Information.

^{1}H NMR spectra were recorded with a Bruker Avance DPX-400, DRX-600, Avance 400 QNP Cryo, or Avance 500 Cryo spectrometer with the residual solvent peak as the internal reference ($CDCl_3$ = 7.26 ppm, [D_6]DMSO = 2.50 ppm). ^{1}H resonances are reported to the nearest 0.01 ppm. ^{13}C NMR Spectra were recorded with the same spectrometers with the central resonance of the solvent peak as the internal reference ($CDCl_3$ = 77.16 ppm, [D_6]DMSO = 39.52 ppm). All ^{13}C resonances are reported to the nearest 0.1 ppm. DEPT 135, COSY, HMQC and HMBC experiments were used to aid structural determination and spectral assignment. The multiplicity of ^{1}H signals are indicated as: s = singlet, d = doublet, t = triplet, m = multiplet, br. = broad, or combinations of thereof. Coupling constants (*J*) are quoted in Hz and reported to the nearest 0.1 Hz. Where appropriate, averages of the signals from peaks displaying multiplicity were used to calculate the value of the coupling constant. IR spectra were obtained by use of a Perkin–Elmer RX1 spectrometer (neat, ATR sampling) with the intensities of the characteristic signals being reported as weak (w, <20 % of tallest signal), medium (m, 21–70 % of tallest signal) or strong (s, > 71 % of tallest signal). Low and high resolution mass spectrometry was performed by using the indicated techniques on either Waters LCT Premier XE or Waters TQD instruments equipped with Acquity UPLC and a lock-mass electrospray ion source. For accurate mass measurements the deviation from the calculated formula is reported in ppm. Melting points were recorded on an Optimelt automated melting point system with a heating rate of 1 °C/min and are uncorrected.

4-Amino-3-isopropylbenzoic Acid (7): Mp 131–132 °C; LC-MS: Rt = 3.63, $[MH]^+$ = 180.25. ^{1}H NMR (400 MHz, [D_6]DMSO): δ = 11.91 (br. s, 1 H), 7.60 (d, *J* = 1.9 Hz, 1 H), 7.48 (dd, *J* = 8.4, 1.9 Hz, 1 H), 6.59 (d, *J* = 8.4 Hz, 1 H), 5.64 (s, 2 H, NH_2), 2.95 (sept., *J* = 6.7 Hz, 1 H), 1.16 (d, *J* = 6.7 Hz, 6 H) ppm. ^{13}C NMR (100 MHz, [D_6]DMSO): δ = 167.7 (C), 150.0 (C), 129.7 (C), 128.3 (CH), 126.8 (CH), 117.3 (C), 113.4 (CH), 26.1 (CH), 22.1 (CH_3) ppm. IR: $\tilde{\nu}$ = 3504.2 (m), 3389.5 (m), 2957.7 (m), 1663.6 (s), 1624.4 (s), 1586.7 (s) cm^{-1}. HRMS: Calcd for $[C_{10}H_{14}NO_2]^+$ = 180.1025, found 180.1030, Δ = 2.8 ppm; The structure was unambiguously confirmed by X-ray crystallography – CCDC reference 1564268.

***N*-(4-Bromo-2-isopropylphenyl)acetamide (8):** Mp 129–132 °C; LC-MS: Rt = 3.84, $[MH]^+$ = 213.97. ^{1}H NMR (400 MHz, [D_6]DMSO): δ = 9.35 (br. s, 1 H, NH), 7.43 (d, *J* = 2.0 Hz, 1 H), 7. 33 (dd, *J* = 8.5, 2.0 Hz, 1 H), 7.24 (d, *J* = 8.5 Hz, 1 H), 3.14 (sept., *J* = 6.8 Hz, 1 H), 2.05 (s, 3 H), 1.18 (d, *J* = 6.8 Hz, 6 H) ppm. ^{13}C NMR (100 MHz, [D_6]DMSO): δ = 168.7 (C), 145.5 (C), 134.3 (C), 128.7 (CH), 128.5 (CH), 128.3 (CH), 118.4 (C), 27.2 (CH_3), 23.1 (CH), 22.8 (CH_3) ppm. IR: $\tilde{\nu}$ = 3244.0 (w br), 2963.4 (m), 1655.4 (s), 1518.6 (s), 1482.3 (s) cm^{-1}. HRMS: Calcd for $[C_8H_9NOBr]^+$ = 213.9868, found 213.9871, Δ = 1.4 ppm; Microanalysis: C = 51.58 % (51.69 %), H = 5.51 % (5.43 %), N = 5.47 % (5.76 %), Br = 31.2 % (31.45 %) The structure was unambiguously confirmed by X-ray crystallography – CCDC reference 1564270.

***N*-(2-Isopropylphenyl)acetamide (9):** Mp 71–73 °C; LC-MS: Rt = 3.72, $[M]^+$ = 177.95. ^{1}H NMR (400 MHz, $CDCl_3$) as a mixture of rotamers a:b (1:3), only the major rotamer is reported: δ = 7.03–7.62 (m, 5 H), 3.17–3.20 (m, 1 H), 2.98–3.03 (m, 1 H), 2.21 (s, 3 H), 1.90 (s, 3 H), 1.20–1.26 (d, *J* = 6.8 Hz, 6 H). ^{13}C NMR (150 MHz, $CDCl_3$): 169.1 (C), 141.1 (C), 134.1 (C), 126.4 (CH), 126.37 (CH), 125.74 (CH), 125.68 (CH), 28.0 (CH_3), 24.1 (CH), 23.2 (CH_3) ppm. IR: $\tilde{\nu}$ = 3278.7 (m), 2964.3 (m), 1676.5 (m), 1655.0 (s), 1515.9 (s), 1489.6 (s) cm^{-1}. HRMS: Calcd for $[C_{11}H_{15}NONa]^+$ = 200.1051, found 200.1044, Δ = 3.5 ppm.

***N*-(4-Cyano-2-isopropylphenyl)acetamide (11):** Mp 134–136 °C; LC-MS: Rt = 3.65, $[M]^-$ = 202.00. ^{1}H NMR (500 MHz, $CDCl_3$): δ = 8.09 (m, 1 H), 7.55 (d, *J* = 1.9 Hz, 1 H), 7.49 (dd, *J* = 8.4, 1.9 Hz, 1 H), 7.22 (br. s, 1 H, NH), 3.12 (sept., *J* = 6.8 Hz, 1 H), 2.24 (s, 3 H), 1.28 (d, *J* = 6.8 Hz, 6 H) ppm. ^{13}C NMR (125 MHz, $CDCl_3$): δ = 168.6 (C), 139.1 (C), 138.6 (C), 130.6 (CH), 129.9 (CH), 123.5 (CH), 119.2 (C), 108.5 (C), 27.9 (CH_3), 24.8 (CH), 22.7 (CH_3) ppm. IR: $\tilde{\nu}$ = 3248.2 (m br), 2985.0 (m), 2225.9 (w), 1709.3 (m), 1645.5 (s), 1519.7 (s) cm^{-1}. HRMS: Calcd for $[C_{12}H_{15}N_2O]^+$ = 203.1184, found 203.1188, Δ = 2.0 ppm. The structure was unambiguously confirmed by X-ray crystallography – CCDC reference 1564264.

Ethyl 4-Acetamido-3-isopropylbenzoate (12): LC-MS: Rt = 4.09, $[MH]^+$ = 250.10, ^{1}H (400 MHz, [D_6]DMSO): 9.46 (s, NH, 1 H), 7.86 (d, *J* = 1.7 Hz, 1 H), 7.74 (dd, *J* = 8.4, 1.7 Hz, 1 H), 7.58 (d, *J* = 8.4 Hz, 1 H), 4.30 (q, *J* = 7.1 Hz, 2 H), 3.26 (sept., *J* = 6.8 Hz, 1 H), 2.09 (s, 3 H), 1.32 (t, *J* = 7.1 Hz, 3 H), 1.17 (d, *J* = 6.8 Hz, 6 H); ^{13}C (400 MHz, [D_6]DMSO): 168.8 (C), 165.5 (C), 141.7 (C), 139.6 (C), 126.7 (C), 126.6 (CH), 123.4 (CH), 125.6 (CH), 60.5 (CH_2), 26.7 (CH), 23.3 (CH_3), 22.9 (CH_3), 14.2 (CH_3). IR: $\tilde{\nu}$ = 3251.3 (m), 2986.2 (m), 1708.6 (s), 1645.9 (s), 1610.1 (m), 1521.1 (s), 1479.6 (m) cm^{-1}. HRMS: Calcd for $[C_{14}H_{20}NO_3]^+$ = 250.1443, found 250.1448, Δ = 2.0 ppm. Microanalysis: C = 67.22 % (67.45 %), H = 7.62 % (7.68 %), N = 5.61 % (5.62 %).

***N*-(4-Carboxy-2-isopropylphenyl)acetamide (13):** White solid; Mp. 214.1–215.8 °C; LC-MS: Rt 1.35, $[MH]^+$ = 222.8, $[2MH]^+$ = 443.5.

^{1}H NMR (400 MHz, [D$_6$]DMSO): δ = 12.83 (s, 1 H), 9.47 (s, 1 H), 7.87 (d, J = 2.1 Hz, 1 H), 7.73 (dd, J = 8.3, 2.1 Hz, 1 H), 7.54 (d, J = 8.3 Hz, 1 H), 3.35 (sept, J = 6.8 Hz, 1 H), 2.10 (s, 3 H), 1.17 (d, J = 6.8 Hz, 6 H) ppm. ^{13}C NMR (101 MHz, [D$_6$]DMSO): δ = 169.34 (C), 167.59 (C), 142.12 (C), 139.74 (C), 128.01 (C), 127.39 (CH), 127.15 (CH), 126.11 (CH), 27.19 (CH$_3$), 23.82 (CH), 23.46 (CH$_3$) ppm. IR: $\tilde{\nu}$ = 3255.9 (m), 2968.9 (m), 2555.6 (br. w), 1688.6 (s), 1645.0 (s), 1607.8 (m), 1581.2 (m), 1520.8 (s) cm^{-1}. HRMS: Calcd for [C$_{12}$H$_{16}$NO$_3$]$^+$ = 222.1130, found 222.1137, Δ = 3.2 ppm.

Methyl 4-Acetamido-3-isopropylbenzoate (14): White solid; Mp. 128.9–130.2 °C; LC-MS: Rt 1.93, [MH]$^+$ = 236.8, [2MH]$^+$ = 471.4. ^{1}H NMR (400 MHz, [D$_6$]DMSO): δ = 9.50 (s, 1 H), 7.89 (d, J = 2.1 Hz, 1 H), 7.76 (dd, J = 8.4, 2.1 Hz, 1 H), 7.60 (d, J = 8.4 Hz, 1 H), 3.84 (s, 3 H), 3.27 (sept, J = 6.8 Hz, 1 H), 2.11 (s, 3 H), 1.17 (d, J = 6.8 Hz, 6 H) ppm. ^{13}C NMR (101 MHz, [D$_6$]DMSO): δ = 169.38 (C), 166.47 (C), 142.12 (C), 140.14 (C), 127.27 (CH), 126.79 (C), 126.97 (CH), 126.09 (CH), 52.42 (CH$_3$), 27.17 (CH$_3$), 23.83 (CH), 23.40 (CH$_3$) ppm. IR: $\tilde{\nu}$ = 3256.2 (m), 2963.4 (w), 1720.2 (s), 1643.7 (s), 1608.1 (m), 1514.0 (s) cm^{-1}. HRMS: Calcd for [C$_{13}$H$_{18}$NO$_3$]$^+$ = 236.1287, found 236.1296, Δ = 3.8 ppm.

***N*-[4-(3-Hydroxy-3-methylbut-1-ynl)-2-isopropylphenyl]acetamide (16):** Off-white solid; Mp. 136.2–137.4 °C; LC-MS: Rt 1.89, [MH]$^+$ = 261.0; Indication of rotameric structure: ^{1}H NMR (400 MHz, CDCl$_3$): δ = 7.78–7.54 (m, 1 H), 7.55–7.40 (m, 1 H), 7.29 (s, 1 H), 7.13 (t, J = 6.0 Hz, 1 H), 2.99 (h, J = 6.8 Hz, 1 H), 2.20–2.05 (br. s, 3 H), 1.65–1.50 (m, 6 H), 1.17 (d, J = 6.8 Hz, 7 H) ppm. ^{13}C NMR (101 MHz, CDCl$_3$): δ = 169.29 (C), 140.92 (C), 134.11 (C), 129.56 (CH), 129.10 (CH), 125.04 (CH), 120.32 (C), 93.54 (C), 82.00 (C), 65.49 (C), 31.50 (CH$_3$), 27.72 (CH$_3$), 23.99 (CH), 22.94 (CH$_3$) ppm. ^{1}H NMR (400 MHz, [D$_6$]DMSO): δ = 9.37 (s, 1 H), 7.34 (d, J = 8.2 Hz, 1 H), 7.27 (d, J = 2.0 Hz, 1 H), 7.17 (dd, J = 8.2, 2.0 Hz, 1 H), 3.17 (sept., J = 6.8 Hz, 1 H), 2.07 (s, 3 H), 1.47 (s, 6 H), 1.14 (d, J = 6.8 Hz, 6 H) ppm. ^{13}C NMR (101 MHz, [D$_6$]DMSO): δ = 169.20 (C), 143.07 (C), 135.54 (C), 129.06 (CH), 128.90 (CH), 126.94 (CH), 120.24 (C), 95.87 (C), 80.92 (C), 64.08 (C), 32.11 (CH$_3$), 27.27 (CH$_3$), 23.68 (CH), 23.43 (CH$_3$) ppm. IR: $\tilde{\nu}$ = 3233.2 (br. m), 2971.9 (m), 1658.5 (s), 1577.9 (w), 1520.2 (s) cm^{-1}. HRMS: Calcd for [C$_{16}$H$_{22}$NO$_2$]$^+$ = 260.1651, found 260.1648, Δ = –1.2 ppm.

***N*-[4-(2,2-Dibromo-3-hydroxy-3-methylbutanoyl)phenyl]acetamide (17):** Pale-brown solid; Mp. 146.2–148.1 °C; LC-MS: Rt 4.70, [MH]$^+$ = 436.1; ^{1}H (400 MHz, [D$_6$]DMSO) 9.50 (s, 1 H), 8.25 (d, J = 2 Hz, 1 H), 8.03 (dd, J = 8.7, 2 Hz, 1 H), 7.58 (d, J = 8.7 Hz, 1 H), 5.55 (br. s, 1 H), 3.27 (sept., J = 6.8 Hz, 1 H), 2.10 (s, 3 H), 1.59 (s, 6 H), 1.17 (d, J = 6.8 Hz, 6 H); ^{13}C ([D$_6$]DMSO) 190.0 (C), 168.5 (C), 140.7 (C), 139.9 (C), 131.1 (C), 129.9 (CH), 129.3 (CH), 124.8 (CH), 80.3 (C), 77.3 (C), 27.6 (CH$_3$), 27.2 (CH$_3$), 24.0 (CH), 23.5 (CH$_3$). IR: $\tilde{\nu}$ = 3431.2 (w), 3368.3 (w), 2160.5 (br. w), 2016.6 (w), 1670 (s), 1598.7 (m), 1578.4 (m), 1506.0 (s), 1473.8 (m), 1456.9 (m), 1374.0 (w), 1356.0 (m), 1259.9 (s), 1211.9 (s), 1184.9 (s) cm^{-1}. HRMS: Calcd for [C$_{16}$H$_{21}$Br$_2$NO$_3$]$^+$ = 432.9888, found 432.9887, Δ = 0.1 ppm. The structure was unambiguously confirmed by X-ray crystallography – CCDC reference 1564265.

4-Ethynyl-2-isopropylaniline (18): Brown oil; LC-MS: Rt = 1.90, [MH]$^+$ = 160.4. ^{1}H NMR (CDCl$_3$): δ = 7.30 (d, J = 1.85 Hz, 1 H), 7.18 (dd, J = 8.1, 1.85 Hz, 1 H), 6.58 (d, J = 8.1 Hz, 1 H), 3.83 (br. s, 2 H, NH$_2$), 2.99 (s, 3 H), 2.83 (sept., J = 6.8 Hz, 1 H), 1.25 (d, J = 6.8 Hz, 6 H) ppm. ^{13}C NMR (CDCl$_3$): δ = 144.7 (C), 132.6 (C), 131.1 (CH), 130.1 (CH), 115.7 (CH), 111.9 (C), 85.4 (C), 75.1 (CH), 28.0 (CH), 22.5 (CH$_3$) ppm. HRMS: Calcd for [C$_{11}$H$_{14}$N]$^+$ = 160.1126, found 160.1126, Δ = 0.0 ppm.

2-Hydroxyisobutyric Acid (19):[43] ^{1}H NMR (400 MHz, [D$_6$]DMSO): δ = 1.25 (s, 3 H) ppm. ^{13}C NMR (101 MHz, [D$_6$]DMSO): δ = 178.32 (C), 71.18 (C), 27.75 (CH$_3$) ppm.

Methyl 2-Hydroxyisobutyrate (20):[44] ^{1}H NMR (400 MHz, [D$_6$]DMSO): δ = 5.30 (br. s, 1 H), 3.61 (s, 3 H), 1.27 (s, 6 H) ppm. ^{13}C NMR (101 MHz, [D$_6$]DMSO): δ = 176.85 (C), 71.55 (C), 52.07 (CH$_3$), 27.72 (CH$_3$) ppm.

Methyl 4-Amino-3-isopropylbenzoate (21): Light-tan solid; Mp. 96.0–97.8 °C; LC-MS: Rt = 2.23, [MH]$^+$ = 194.7. ^{1}H NMR (400 MHz, CDCl$_3$): δ = 7.87 (d, J = 2.0 Hz, 1 H), 7.74 (dd, J = 8.3, 2.0 Hz, 1 H), 6.66 (d, J = 8.3 Hz, 1 H), 4.12 (br. s, 2 H), 3.88 (s, 3 H), 2.87 (sept., J = 6.8 Hz, 1 H), 1.30 (d, J = 6.8 Hz, 6 H) ppm. ^{13}C NMR (101 MHz, CDCl$_3$): δ = 167.53 (C), 147.96 (C), 131.33 (C), 128.82 (CH), 127.59 (CH), 119.95 (C), 114.64 (CH), 51.58 (CH$_3$), 27.61 (CH), 22.03 (CH$_3$) ppm. IR: $\tilde{\nu}$ = 3468.6 (m), 3367.6 (m), 3247.0 (w), 2954.8 (m), 1671.2 (s), 1601.5 (s), 1508.6 (m) cm^{-1}. HRMS: Calcd for [C$_{11}$H$_{16}$NO$_2$]$^+$ = 194.1181, found 194.1190, Δ = 4.6 ppm.

4-Carboxy-2-isopropylbenzenediazonium Chloride (22): ^{1}H NMR (400 MHz, [D$_6$]DMSO): δ = 8.92 (d, J = 8.5 Hz, 1 H), 8.27 (d, J = 1.8 Hz, 1 H), 8.25 (dd, J = 8.5, 1.8 Hz, 2 H), 3.51 (sept., J = 6.7 Hz, 1 H), 1.37 (d, J = 6.7 Hz, 6 H) ppm.

2-[2-(4-Carboxy-2-isopropylphenyl)hydrazinyl]-2-oxoacetic Acid (23): Yellow solid; Mp. 147.5 °C decomposition; LC-MS: Rt = 0.97, [MH]$^+$ = 267.3. ^{1}H NMR (600 MHz, [D$_6$]DMSO): δ = 12.2 (br. s, 1 H), 10.35 (br. s, 1 H), 7.77 (s, 1 H), 7.67 (d, J = 1.5 Hz, 1 H), 7.58 (dt, J = 8.5, 1.5 Hz, 1 H), 6.62 (dd, J = 8.5, 1.5 Hz, 1 H), 3.09 (sept., J = 7.1 Hz, 1 H), 1.21–1.11 (d, J = 7.1 Hz, 6 H) ppm. ^{13}C NMR (101 MHz, [D$_6$]DMSO): δ = 168.02 (C), 162.61 (C), 162.58 (C), 149.51 (C), 131.35 (C), 128.79 (CH), 126.78 (CH), 120.68 (C), 110.71 (CH), 26.33 (CH), 22.81 (CH$_3$) ppm. IR: $\tilde{\nu}$ = 3254.2 (br. m), 2972 (m), 1667.3 (s), 1606.2 (s), 1520.1 (m) cm^{-1}. HRMS: Calcd for [C$_{12}$H$_{15}$N$_2$O$_5$]$^+$ = 267.0981, found 267.0993, Δ = 4.5 ppm.

2-(4-Carboxy-2-isopropylphenyl)hydrazin-1-ium Chloride (24): Light-tan solid; Mp. > 260 °C decomp.; LC-MS: Rt = 3.50, [MH]$^+$ = 221.1; ^{1}H (500 MHz, [D$_6$]DMSO): 12.55 (br. s, 1 H), 10.32 (br. s, 1 H), 8.40 (s, 1 H), 7.78 (d, J = 1.9 Hz, 1 H), 7.76 (dd, J = 8.4, 1.9 Hz, 1 H), 6.97 (d, J = 8.4 Hz, 1 H), 3.15 (sept., J = 6.8 Hz, 1 H), 1.19 (d, J = 6.8 Hz, 6 H). ^{13}C (125 MHz, [D$_6$]DMSO): 167.2 (C), 145.7 (C), 134.1 (C), 128.0 (CH), 126.5 (CH), 123.5 (C), 112.0 (CH), 26.0 (CH), 22.4 (CH$_3$). IR: $\tilde{\nu}$ = 3314.9 (w), 3196.2 (w), 2871.3 (br. m), 1687.1 (s), 1609.4 (s), 1507.1 (m), 1278.6 (s) cm^{-1}. HRMS: Calcd for [C$_{10}$H$_{10}$N$_2$O$_2$Na]$^+$ = 221.1266, found 221.1266, Δ = 0.0 ppm.

4-[5-(2,6-Dimethoxyphenyl)-3-(ethoxycarbonyl)-1*H*-pyrazol-1-yl]-3-isopropylbenzoic Acid (25): Mp: 218–220 °C. ^{1}H NMR (400 MHz, CDCl$_3$): δ = 7.97 (d, J = 1.8 Hz, 1 H), 7.85 (dd, J = 1.8, 8.2 Hz, 1 H), 7.41 (d, J = 8.2 Hz, 1 H), 7.23 (t, J = 8.4 Hz, 1 H), 6.96 (s, 1 H), 6.45 (d, J = 8.4 Hz, 2 H), 4.44 (q, J = 7.1 Hz, 2 H), 3.63 (s, 6 H), 2.77 (sept., J = 6.7 Hz, 1 H), 1.40 (t, J = 7.1 Hz, 3 H) 1.00 (br. s, 6 H) ppm. ^{13}C NMR (100 MHz, CDCl$_3$): δ = 171.2 (C), 162.8 (C), 158.4 (C), 146.4 (C), 144.3 (C), 142.5 (C), 138.9 (C), 131.6 (CH), 129.9 (C), 128.8 (CH), 128.6 (CH), 127.1 (CH), 111.5 (CH), 106.8 (C), 103.6 (CH), 61.1 (CH$_3$), 55.6 (CH$_2$), 27.8 (CH), 24.1 (CH$_3$), 14.6 (CH$_3$) ppm. IR: $\tilde{\nu}$ = 2400–3300 (w br), 1713.9 (s), 1607.6 (m), 1589.9 (m), 1477.1 (m), 1229.1 (s) cm^{-1}. HRMS: Calcd for [C$_{24}$H$_{27}$N$_2$O$_6$]$^+$ = 439.1869, found 439.1865, Δ = 0.9 ppm. The structure was unambiguously confirmed by X-ray crystallography – CCDC reference 1564267.

CCDC 1564268 (for **7**), 1564270 (for **8**), 1564264 (for **11**), 1564265 (for **17**), 1564267 (for **25**) contain the supplementary crystallographic data for this paper. These data can be obtained free of charge from The Cambridge Crystallographic Data Centre.

Acknowledgments

We are greatful for financial support from the Royal Society (to M. B. and I. R. B.; UF130576 and UF150536 to M. O. K.). We would also like to thank Dr. John Davies and Dr. Andrew D. Bond at the Department of Chemistry, University of Cambridge for solving the X-ray structures of compounds **7**, **8**, **11**, **17**, **25**, **8a** and **12a** (see the Supproting Information for details).

Keywords: Continuous flow · Flow chemistry · Ozonolysis · Cross-coupling · Multi-step synthesis · Synthetic methods

[1] a) R. Carraway, R. S. E. Leeman, *J. Biol. Chem.* **1973**, *248*, 6854–6861; b) W. H. Rostène, M. J. Alexander, *Front. Neuroendocrinol.* **1997**, *18*, 115–173.
[2] E. Popp, A. Schneider, P. Vogel, P. Teschendorf, B. W. Böttigera, *Neuropeptides* **2007**, *41*, 349–354.
[3] P. R. Dobner, *Peptides* **2006**, *240*, 2405–2414.
[4] D. Zhao, C. Pothoulakis, *Peptides* **2006**, *27*, 24234–2444.
[5] P. Kitabgi, *Neurochem. Int.* **1989**, *14*, 111–119.
[6] a) G. Bissette, C. B. Nemeroff, M. W. Decker, J. S. Kizer, Y. Agid, F. Javoy-Agid, *Ann. Neurology* **1985**, *17*, 324–328; b) G. Chinaglia, A. Probst, J. M. Palacios, *Neuroscience* **1990**, *39*, 351–360; c) F. St-Gelais, C. Jomphe, L.-É. Trudeau, *J. Psychiatry Neurosci.* **2006**, *31*, 229–245; d) L. Ferraro, S. Beggiato, D. O. Borroto-Escuela, L. Ravani, W. T. O'Connor, M. C. Tomasini, A. C. Borelli, L. F. Agnati, T. Antonelli, S. Tanganelli, K. Fuxe, *Curr. Protein Pept. Sci.* **2014**, *15*, 681–690.
[7] M. Ocejo-García, S. I. Ahmed, J. M. Coulson, P. Woll, *J. Lung Cancer* **2001**, *33*, 1–9.
[8] F. Souazé, S. Dupouy, V. Viardot-Foucault, E. Bruyneel, S. Attoub, C. Gespach, A. Gompel, P. Forgez, *Cancer Res.* **2006**, *66*, 6243–6249.
[9] J. C. Reubi, B. Waser, H. Friess, M. Buchler, J. Laissue, *Gut* **1998**, *42*, 546–555.
[10] R. R. Giorgi, T. Chile, A. R. Bello, R. Reyes, M. A. H. Z. Fortes, M. C. Machado, V. A. Cescato, N. R. Musolino, M. D. Bronstein, D. Giannella-Neto, M. L. Corrêa-Giannella, *J. Neuroendocrinol.* **2008**, *20*, 1052–1057.
[11] P. Schaeffer, M. C. Laplace, A. Bernat, V. Prabonnaud, D. Gully, L. Lespy, J. M. Herbert, *J. Cardiovasc. Pharmacol.* **1998**, *31*, 545–550.
[12] P. Kitabgi, F. De Nadai, C. Rovère, J. N. Bidard, *Ann. N. Y. Acad. Sci.* **1992**, *668*, 30–42.
[13] G. A. Cain, T. E. Christos, A. L. Johnson, R. S. Pottorf, P. N. Confalone, S. W. Tam, W. K. Schmidt, *Bioorg. Med. Chem. Lett.* **1993**, *3*, 2055–2060.
[14] a) C. Battilocchio, B. J. Deadman, N. Nikbin, M. O. Kitching, I. R. Baxendale, S. V. Ley, *Chem. Eur. J.* **2013**, *19*, 7917–7930; b) I. R. Baxendale, S. Cheung, M. O. Kitching, S. V. Ley, J. W. Shearman, *Bioorg. Med. Chem.* **2013**, *21*, 4378–4387.
[15] C. Betancur, M. Canton, A. Burgos, B. Labeeuw, D. Gully, W. Rostène, D. Pelaprat, *Eur. J. Pharmacol.* **1998**, *343*, 67–77.
[16] a) B. J. Deadman, S. V. Ley, D. L. Browne, I. R. Baxendale, *Chem. Eng. Technol.* **2015**, *38*, 259–264; b) C. Battilocchio, I. R. Baxendale, M. Biava, M. O. Kitching, S. V. Ley, *Org. Process Res. Dev.* **2012**, *16*, 798–810.
[17] The thermal contact between the 3 mixing chips was ensured using a layer of Akasa AK-450 silver based thermal compound (thermal conductivity: 9.24 W/m °C).
[18] Biotage universal separator part number 120–1930-V. During prolonged operation the membrane efficiency was noted to decrease. A duplicate set-up was switched to allowing cleaning of the membrane. In most cases a simple back flushing of the membrane with 4:1 mixture of DCM/MeOH followed by vacuum drying reconditioned the membrane.
[19] J. A. Souto, R. A. Stockman, S. V. Ley, *Org. Biomol. Chem.* **2015**, *13*, 3871–3877.
[20] For a review of palladium catalysis in synthesis, see: C. C. C. J. Seechurn, M. O. Kitching, T. J. Colacot, V. Snieckus, *Angew. Chem. Int. Ed.* **2012**, *51*, 5062–5085; *Angew. Chem.* **2012**, *124*, 5150.
[21] See: M. R. Pitts, P. McCormack, J. Whittall, *Tetrahedron* **2006**, *62*, 4705–4708. Poly(methylhydrosiloxane), CAS Number: 63148–57–2; Ave. Mn 1,700–3,200 available from Aldrich.
[22] a) C. J. Mallia, I. R. Baxendale, *Org. Process Res. Dev.* **2016**, *20*, 327–360; b) C. J. Mallia, G. C. Walter, I. R. Baxendale, *Beilstein J. Org. Chem.* **2016**, *12*, 1503–1511; c) T. Fukuyama, T. Totoki, I. Ryu, *Green Chem.* **2014**, *16*, 2042–2050.
[23] Brukhurst HIGH-TECH EL-FLOW® flow meter/controller available from http://www.bronkhorst.co.uk/.
[24] Gilson 307 HPLC pump installed with a SC.5 10 mL pump head.
[25] Polar Bear Plus flow coil reactor. Available from Cambridge Reactor Design. http://www.cambridgereactordesign.com/.
[26] Knauer back-pressure regulator adjustable back-pressure regulator controlled between 1-20 bar. Product code: A70087. http://www.knauer.net.
[27] GE Healthcare life sciences PTFE (polytetrafluoroethene) solvent filter; product code: 11-0007-68. http://www.gelifesciences.com.
[28] Advantec MFS PTFE (polytetrafluoroethene) extraction thimble filter No. 89, 22 × 25 × 90 mm. product code: 1177C34. http://www.advantecmfs.com.
[29] a) W. P. Griffith, A. G. Shoair, M. Suriaatmaja, *Synth. Commun.* **2000**, *30*, 3091–3095; b) D. Yang, F. Chen, Z.-M. Dong, D.-W. Zhang, *J. Org. Chem.* **2004**, *69*, 2221–2223.
[30] T. Fukuyama, Md. T. Rahman, Y. Sumino, I. Ryu, *Synlett* **2012**, *23*, 2279–2283.
[31] A small amount (1.2–3 %) of the fully deprotected acetylene **18** was also detected after prolonged stirring.
[32] J. Zak, D. Ron, E. Riva, H. P. Harding, B. C. S. Cross, I. R. Baxendale, *Chem. Eur. J.* **2012**, *18*, 9901–9910.
[33] a) S. Jackson, H. A. Hull, *J. Org. Chem.* **1976**, *41*, 3340–3342; b) C. Hurd, R. D. Christ, *J. Org. Chem.* **1936**, *1*, 141–145; c) E. Dallwigk, H. Paillard, E. Briner, *Helv. Chim. Acta* **1952**, *35*, 1377–1384; d) P. S. Bailey, Y.-G. Chang, W. Kwie, *J. Org. Chem.* **1962**, *27*, 1198–1201; e) W. B. DeMore, C.-L. Lin, *J. Org. Chem.* **1973**, *38*, 985–989; f) D. J. Miller, T. E. Nemo, L. A. Hull, *J. Org. Chem.* **1975**, *40*, 2675–2678; g) K. Griesbaum, Y. Dong, *Liebigs Ann./Recueil* **1997**, *4*, 753–756; h) A. V. Maiorov, B. E. Krisyuk, A. A. Popov, *Khimicheskaya Fizika* **2008**, *27*, 62–65; i) S. E. Wheeler, D. H. Ess, K. N. Houk, *J. Phys. Chem. A* **2008**, *112*, 1798–1807.
[34] It appeared from a basic evaluation of the limited substrate scope that aliphatic substituted acetylenes gave the corresponding anhydrides or acids (in the presence of water) whereas diaryl acetylenes i.e. from diphenylacetylene produced the corresponding benzoin. However this was contradicted in several papers based upon the same substrate.
[35] For other examples of continuous ozonolysis, see: a) M. D. Roydhouse, W. B. Motherwell, A. Coustaninou, A. Gavriilidis, R. Wheeler, K. Down, I. Campbell, *RSC Adv.* **2013**, *3*, 5076–5082; b) N. Steinfeldt, R. Abdallah, U. Dingerdissen, K. Jähnisch, *Org. Process Res. Dev.* **2007**, *11*, 1025–1031; c) N. Steinfeldt, U. Bentrup, K. Jähnisch, *Ind. Eng. Chem. Res.* **2010**, *49*, 72–80; d) S. Hübner, U. Bentrup, K. Budde, T. Lovis, A. Dietrich, L. Freitag, K. Jähnisch, *Org. Process Res. Dev.* **2009**, *13*, 952–960; e) M. O'Brien, I. R. Baxendale, S. V. Ley, *Org. Lett.* **2010**, *12*, 1596–1598; f) M. Irfan, T. N. Glasnov, C. O. Kappe, *Org. Lett.* **2011**, *13*, 984–987.
[36] a) Y. Taitel, A. E. Dukler, *AIChE J.* **1976**, *22*, 47–55; b) E. Trononi, *AIChE J.* **1990**, *36*, 701–709; c) H. M. Soliman, *Can. J. Chem. Eng.* **1982**, *60*, 475–481.
[37] Quantofix® peroxides test sticks available from Sigma Aldrich cat. no. Z101680. Range 0, 0.5, 2, 5, 10, 25 mg/L.
[38] a) Z. Yu, G. Tong, X. Xie, P. Zhou, Y. Lv, W. Su, *Org. Process Res. Dev.* **2015**, *19*, 892–896; b) B. Li, D. Widlicka, S. Boucher, C. Hayward, J. Lucas, J. C. Murray, B. T. O'Neil, D. Pfisterer, L. Samp, J. VanAlsten, Y. Xiang, Y. Young, *J. Org. Process Res. Dev.* **2012**, *16*, 2031–2035; c) L. Malet-Sanz, J. Madrzak, S. V. Ley, I. R. Baxendale, *Org. Biomol. Chem.* **2010**, *8*, 5324–5332.
[39] a) D. L. Browne, I. R. Baxendale, S. V. Ley, *Tetrahedron* **2011**, *67*, 10296–10303 (and references therein) b) T. Hu, I. R. Baxendale, M. Baumann, *Molecules* **2016**, *21*, 918–941; c) J.-S. Poh, D. L. Browne, S. V. Ley, *React. Chem. Eng.* **2016**, *1*, 101–105.
[40] Oxamic acids such as compound **24** have been shown to be synthetic equivalents to hydrazine readily deprotecting under thermal conditions; for selected examples, see: a) J. F. Lambert, T. Norris, Patent Int. Appl., 2002044133, **2002**; b) T. Norris, C. Bezze, S. Z. Franz, M. Stivanello, *Org. Process Res. Dev.* **2009**, *13*, 354–357; c) C. P. Ashcroft, P. Hellier, A. Pettman, S. Watkinson, *Org. Process Res. Dev.* **2011**, *15*, 98–103; d) M. Marinozzi, G. Marcelli, A. Carotti, B. Natalini, *RSC Adv.* **2014**, *4*, 7019–7023.
[41] Commercially available from Vapourtec. https://www.vapourtec.com/.

[42] We believe based upon analysis of samples that a significant proportion of the 2-hydroxyisobutyric acid decomposes to CO and acetone under the acidic conditions used in the preparation of **22** simplifying work up. This type of reaction is known in the literature but normally requires an activator: a) R. A. Singh, A. Kumar, *Oxidation Commun.* **2013**, *36*, 965–972; b) G. E. M. Moussa, M. E. Shaban, F. A. Fouli, A. N. Hegazi, *J. Chem. Soc. Pak.* **1987**, *9*, 239–244. It does however resemble the acid promoted oxidation of malic acid to coumaric acid see: c) H. E. Zimmerman, G. L. Grunewald, R. M. Paufler, *Org. Synth.* **1966**, *46*, 101–104; d) I. W. Ashworth, M. C. Bowden, B. Dembofsky, D. Levin, W. Moss, E. Robinson, N. Szczur, J. Virica, *Org. Process Res. Dev.* **2003**, *7*, 74–81; e) I. R. Baxendale, M. Baumann, *Beilstein J. Org. Chem.* **2013**, *9*, 2265–2319.

[43] K. Watanabe, Y. Andou, Y. Shirai, H. Nishida, *Chem. Lett.* **2010**, *39*, 698–699.

[44] G. M. Rubottom, R. Marrero, *Synth. Commun.* **1981**, *11*, 505–511.

Received: June 24, 2017

